

# Optimizing Design of Smaller Antennas for Proximity Transponders

Michael Gebhart

System and Analog Innovation  
NXP Semiconductors  
Gratkorn, Austria  
gebhart@ieee.org

Reinhard Szoncsó

Customer Application Service  
NXP Semiconductors  
Gratkorn, Austria  
Reinhard.Szoncsó@nxp.com

**Abstract**—New person-related applications now require to produce 13.56 MHz SmartCard transponders supporting the ISO/IEC14443 Proximity Standard in smaller sizes. We describe antenna design methods in combination with transponder system properties, to show how to efficiently combine established chip platforms with smaller antenna form factors.

**Keywords**—Contactless Technology, Loop Antennas, SmartCards, ISO/IEC14443.

## I. INTRODUCTION

Today, a huge amount of personal cards are in practical use, with an increasing focus on applications requiring higher security. Near Field Contactless technology was implemented as a comfortable interface for the user and world-wide standardized one decade ago in the ISO/IEC14443 Proximity Standard. This enables electronic passports, contactless credit cards, access control or public transport ticketing as successful solutions being part of our daily life. The typical format of such cards is ID-1, specified in ISO/IEC7810. Fig. 1 gives a simplified impression of ID-1, and as can be seen, there are other characteristics which may be part of the card. Examples shown are the magnetic stripe, a contact interface to a microchip, or embossing, which means letters raised in relief for character recognition.

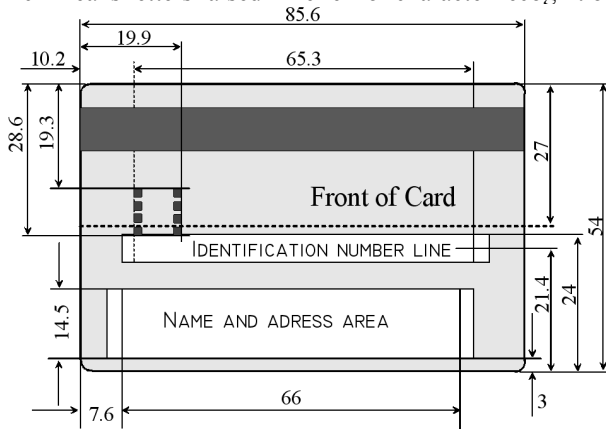


Figure 1. Card geometry specifications in millimeters.

As it is not possible to place antenna turns below embossed areas or below a contact interface in reliable production processes, this restricts the area which can be used for the transponder loop antenna. Also, there must be a distance of about 3 mm to the card border to allow lateral

tolerances in the position of different polymer sheets in card production and to avoid delamination of the structure. Therefore, smaller antennas are required. This holds especially for contactless credit cards (featuring four-line embossing), so-called stickers with ferrite for payment applications and seal authentication, or objects like watches, which must use smaller antennas due to their limited size. It is the objective to combine such smaller antenna sizes with well established transponder chip platforms featuring high security and performance for person related applications. ISO/IEC14443 defines properties at the air interface, and existing reader infrastructure was built to meet these requirements. For smaller antennas to achieve similar properties as with a class 1 antenna (which is used for most high volume applications to date) is the challenge for efficient antenna design.

## II. LOOP ANTENNA DESIGN

The analogue performance of a transponder from a system perspective can be considered by a simplified equivalent circuit given in fig. 2.

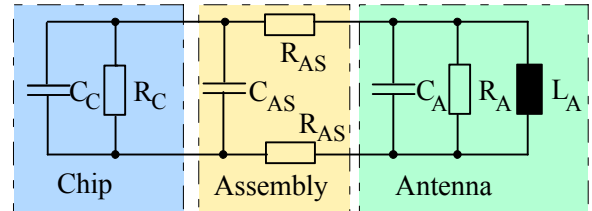


Figure 2. Contactless SmartCard electrical system equivalent circuit.

In this circuit, the chip properties are represented by an equivalent input capacitance  $C_C$ , and a resistance  $R_C$ , which represents the power dissipated in chip operation with a constant, limited voltage. The assembly of the chip to the antenna may add additional losses  $R_{AS}$  (however depending on the technology, this can be negligible) and an additional, small capacitance  $C_{AS}$  depending on the chip package. The antenna is represented by a parallel resonant circuit, consisting of inductance  $L_A$ , capacitance  $C_A$  and resistance  $R_A$ .

Several publications are available, which describe different aspects for loop antenna design, starting with Maxwell [1], who gives analytical equations for inductance of some special cases, to [2], which presents many useful approximations for practical cases in RFID applications, to [3] – [11]. However, one uncertainty are unknown material

properties and border effects, which can require a more practical approach:

Loop antenna design will start with an antenna geometry defined by the intended application and try to achieve target values for the equivalent electrical circuit. The main parameter is the inductance, less important are the parasitic capacitance, and the antenna losses, represented by the resistance. In this context it is currently state of the art to use analytical formulas for an approximation of the parameters, which is sufficiently accurate to allow production. For more precise results, usually a matrix of varied geometry parameters is produced and subsequently measured, then the model is fitted to specific material or process properties (e.g. dielectric losses of polymers are not always known exactly).

#### A. Antenna Inductance estimation

In a first step, the geometry of the rectangular loop antenna consisting of several turns (as shown as sample designs in fig. 3 and 4) is converted to the geometry of a single turn. The rectangular conductor cross-section is approximated with a circular cross-section of equal area

$$d = 2\sqrt{\frac{t \cdot w}{\pi}} \quad (1)$$

where  $d$  is the equivalent circular conductor diameter,  $w$  is the rectangular conductor track width, and  $t$  the conductor thickness (all dimensions in millimeters). We use the square mean to calculate the average length  $a$  and the average width  $b$  of a single turn rectangular loop out of the maximum length  $a_0$  and the maximum width  $b_0$  of the antenna.  $g$  specifies the gap between conductor tracks and  $N$  is the number of turns.

$$a = \sqrt{\frac{a_0^2 + [a_0 - 2N \cdot (g + w)]^2}{2}} \quad (2)$$

$$b = \sqrt{\frac{b_0^2 + [b_0 - 2N \cdot (g + w)]^2}{2}} \quad (3)$$

The inductance of this single turn loop coil consists of contributions for self-inductance  $L_1$  and  $L_2$  given in eq. (4) and (5), which only depend on the conductor length and magnetic constant  $\mu_0$ , and of mutual inductance  $M_1$  and  $M_2$  between all parallel conductor parts, given in eq. (6) and (7).

$$L_1 = \frac{\mu_0 \cdot a}{16\pi} \quad (4), \quad \text{and} \quad L_2 = \frac{\mu_0 \cdot b}{16\pi}. \quad (5)$$

$$M_1 = \frac{\mu_0}{2\pi} \left[ a \cdot \ln \left( \frac{2 \cdot a \cdot b}{d \cdot (a + \sqrt{a^2 + b^2})} \right) - 2b + \sqrt{a^2 + b^2} \right] \quad (6)$$

$$M_2 = \frac{\mu_0}{2\pi} \left[ b \cdot \ln \left( \frac{2 \cdot a \cdot b}{d \cdot (b + \sqrt{a^2 + b^2})} \right) - 2a + \sqrt{a^2 + b^2} \right] \quad (7)$$

All terms are summarized for the inductance of the complete loop. To take into account the number of turns  $N$ , this sum is multiplied by  $N$  to the power of  $E$ . To compensate edge effects and take a radius and bridge crossing into account,  $E$  is set to 1.64 for the designs given in

fig. 3 and 4.  $L_A$  is the antenna inductance in microhenry.

$$L_A = (2M_1 + 2M_2 + 2L_1 + 2L_2) \cdot N^E \quad (8)$$

We will use two designs as practical examples:

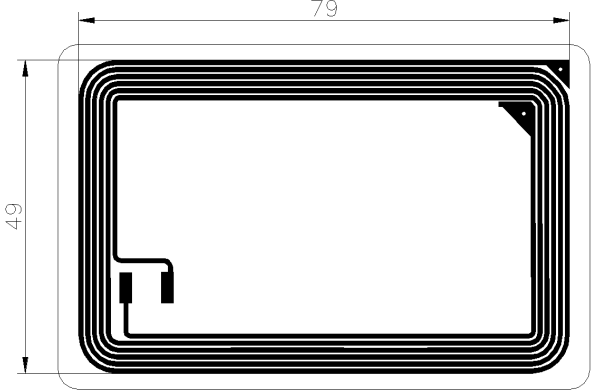


Figure 3. Full size (class 1) etched antenna layout.

TABLE I. MEASURED CLASS 1 ANTENNA PARAMETERS

Antenna geometry (mm)		Electrical parameters	
outline	79 x 49	Inductance	4.75 $\mu$ H
track width	0.7	Capacitance	3.93 pF
track gap	0.4	DC-Resistance	2.55 $\Omega$
thickness	0.018	$R_A (@13.56)$	50 k
turns	6	Q-factor	$\sim 124$

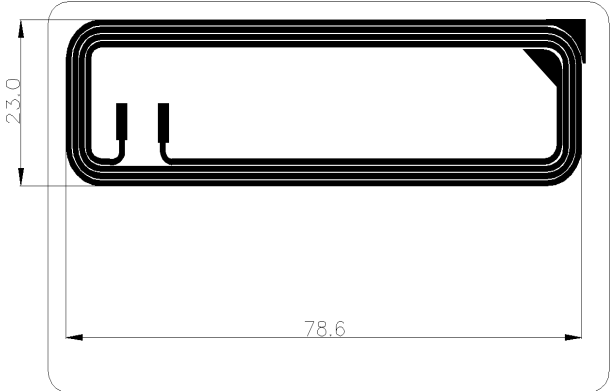


Figure 4. Half size (class 2) etched antenna layout.

TABLE II.

Antenna geometry (mm)		Electrical parameters	
outline	78.6 x 23	Inductance	1.64 $\mu$ H
track width	0.8	Capacitance	3.74 pF
track gap	0.2	DC-Resistance	0.65 $\Omega$
thickness	0.035	$R_A (@13.56)$	22 k
turns	4	Q-factor	$\sim 155$

#### B. Antenna resistance estimation

Antenna losses are the result of DC-resistance and losses due to the skin effect. The serial conductor DC-resistance in

Ohm for a planar spiral antenna can be estimated by

$$R_{DC} = \frac{2N(a_0 + b_0) - 2(N-1)(w+g)}{\sigma \cdot t \cdot w \cdot \text{factor}} \quad (10)$$

where  $\sigma$  is the track conductance, e.g.  $5.8 \cdot 10^{-7} \text{ Sm}^{-1}$  for copper. A factor (close to  $0.9 \cdot 10^{-3}$  for all dimensions in mm) can take into account edge radius and production tolerances. Skin effect losses are difficult to estimate, a low-frequency approximation for the AC-resistance is given by

$$R_{AC} \approx R_{DC} \left[ 1 + \frac{(d \cdot 10^{-3})^2 \cdot f \pi \mu_0 \sigma}{4.48} \right] \quad (11)$$

where  $f$  is the operating frequency. The equivalent parallel resistance  $R_A$  can be calculated from serial resistance according to

$$R_A = \frac{(2\pi f L_A \cdot 10^{-6})^2}{R_{SERIAL}}. \quad (12)$$

Target criterion is that antenna losses, represented by  $R_A$ , should be at least a magnitude smaller than chip losses, represented by  $R_C$ , so that the optimum achievable performance is not degraded significantly. For constant voltage operation, this means  $R_A \geq 10 R_C$  so that  $R_T \approx R_C$ .

### C. Industrial production technologies

Four industrial production technologies are available today for antenna and inlay production: Etched antennas, embedded wire, galvano and printed antennas. Not all electrical characteristics can be achieved with each technology, but the selection of the technology may already be defined by the final product or the application. Low losses, for example, can be achieved with etched, embedded wire and also galvano antennas, so a high antenna Q-factor can be achieved.  $Q_A$  can be calculated by

$$Q_A = \frac{R_A}{2\pi f_{RES} L_A} \quad (13)$$

and should not be confused with the Q-factor of the whole transponder,  $Q_T$ , which is given by

$$Q_T = \frac{\frac{R_A R_C}{R_A + R_C}}{2\pi f_{RES} L_A} \approx \frac{R_T}{2\pi f_{RES} L_A}. \quad (14)$$

Significant capacitance, on the other hand, can be integrated in etched, printed and galvano-antennas for double-sided constructions e.g. in conductor-crossings.

Once more it should be mentioned, all these equations mentioned in chapter II are approximations, useful to estimate values for antenna design. Uncertainties exist for material parameters or for example the edge construction in rectangular loops, and the track gap, which influence the parameter  $E$  in the inductance. In case the geometry and material properties are very well known, field simulation software like HFSS, CST or ADS / Momentum can be used, if available. However, analytical approximations also are useful to extend the considerations given in the next section.

### III. TRANSPONDER PROPERTIES AT THE AIR INTERFACE

The basic properties of a transponder are the minimum H-field required for operation, reader command demodulation, and card loading and load modulation amplitude. As the 2nd requirement is depending on chip internal demodulation and decoding (and signal distortion caused by the transponder Q-factor), we will focus on the required H-field strength and the emitted load modulation strength.

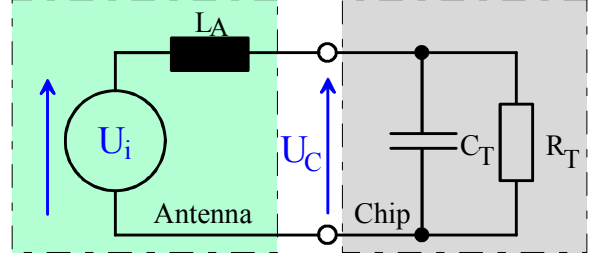


Figure 5. Equivalent Transponder circuit for energy considerations.

#### A. Energy aspects

Considering the energy aspects, the circuit of fig. 2 can be simplified to an equivalent circuit given in fig. 5. For assembly technologies like welding, crimping or soldering we can neglect the assembly resistance, and the additional capacitance will be  $< 1 \text{ pF}$  for contactless chip modules (of typically  $8 \times 5 \text{ mm}$ ). We can summarize antenna and chip components to one parallel resonant circuit and introduce a voltage source to the inductance, to represent the voltage induced by the alternating  $13.56 \text{ MHz}$  H-field. This induced voltage  $u_i(t)$  in a conductor loop is the derivative of the magnetic flux  $\Phi(t)$  normal to the antenna area.

$$u_i(t) = -\frac{d\Phi(t)}{dt} \quad (15)$$

Since the  $90^\circ$  phase shift of the carrier signal is not relevant for our consideration, the voltage amplitude (root mean square value, RMS) is given by

$$U_i = \Phi \cdot \omega_{CAR} = [B \cdot A_{TOT}] \cdot \omega_{CAR} = [(\mu_0 \cdot H) \cdot (N \cdot A)] \cdot (2\pi f_{CAR}) \quad (16)$$

where  $B$  is the magnetic flux density,  $\omega_{CAR}$  is the radian carrier frequency, and  $\mu_0$  is the magnetic constant  $\mu_0 = 4\pi 10^{-7} \text{ Vs/Am}$ . As we are considering resonant circuits, maybe the most interesting parameter is the quality factor  $Q$ . It is defined as the energy  $W$  stored in the system during one signal period, relative to the power loss  $P$ .

$$Q = \frac{\omega W}{P} = \frac{\omega C U_{C,RMS}^2}{P} = \frac{\omega L I_{L,RMS}^2}{P} \quad (17)$$

For the complete transponder system (chip + antenna) we can define a system quality factor  $Q_T$ , which for the case of resonance frequency  $f_{RES}$  equal to carrier frequency  $f_{CAR}$  allows us to re-write the equation for induced voltage amplitude to

$$U_i = \mu_0 \cdot H \cdot N \cdot A \cdot \omega \cdot Q_T. \quad (18)$$

Using the network function for fig. 5, we can express

$$U_C = U_i \cdot \frac{\frac{R_T}{sR_T C_T + 1}}{sL_A + \frac{R_T}{sR_T C_T + 1}}. \quad (19)$$

We can re-arrange the expression and use  $s \rightarrow j\omega$ .

$$U_C = U_i \cdot \frac{1}{1 + j\omega \frac{L_A}{R_T} - \omega^2 L_A C_C} \quad (20)$$

$$\text{With } L_A C_C \equiv \frac{1}{\omega_{RES}^2} \quad (21) \text{ and } \frac{L_A}{R_T} \equiv \frac{1}{\omega_{RES} \cdot Q_T} \quad (22)$$

results for the voltage amplitudes for all resonance frequencies

$$U_C = U_i \cdot \frac{1}{j \frac{\omega_{CAR}}{\omega_{RES}} \cdot \frac{1}{Q_T} + \left(1 - \frac{\omega_{CAR}^2}{\omega_{RES}^2}\right)} \quad (23)$$

which also includes the special case of (18).

If we substitute  $\frac{1}{Q_T} = \frac{2\pi f_{RES} L_A}{R_T}$  (24) and use (16), we

can re-arrange (23) to get a requirement for the minimum H-field to achieve the absolute value of the minimum voltage amplitude for start of chip operation  $U_{MIN}$  at the antenna connection, depending on resonance frequency and other equivalent electrical transponder parameters.

$$H_{MIN} \equiv \frac{\sqrt{\left[1 - \left(\frac{f_{CAR}}{f_{RES}}\right)^2\right]^2 + \left(\frac{2\pi f_{CAR} L_A}{R_P}\right)^2}}{2\pi f_{CAR} \mu_0 N A} \cdot U_{MIN} \quad (25)$$

This can be used to evaluate the energy requirements for given chip characteristics and antenna characteristics. To note, we consider a voltage source representing induction by the reader H-field emission, which means we do not take into account any detuning to the reader. In fact this is consistent with the test methods described in the ISO/IEC10373-6 Standard, which require to compensate the reduction of H-field emission of the transmit antenna by detuning caused by close coupling to the transponder (so-called "card loading effect") by an appropriate increase in the RF amplifier gain.

In fact, this is a very useful expression for many practical considerations for SmartCard transponders operating in voltage limitation by shunt regulation. As one example, we can re-arrange (25) to calculate the allowable resonance frequency limits (maximum and minimum) to meet a required minimum H-field for operation, for certain chip and antenna characteristics. The condition is given by

$$f_{LIM} = \frac{f_{CAR}}{\sqrt{1 \pm \sqrt{\left(\frac{H_{MIN} 2\pi f_{CAR} \mu_0 N A}{U_{MIN}}\right)^2 - \left(\frac{2\pi f_{CAR} L_A}{R_P}\right)^2}}} \quad (26)$$

Consequently this allows to estimate allowable total tolerances for chip capacitance  $C_C$  and antenna inductance  $L_A$  (the two most relevant parameters), very important for mass product applications.

Another aspect is to consider the current, which can be available from the antenna for the SmartCard chip. In case the operation starts if the limited voltage is achieved, we can calculate this current (as function of H and other parameters), if we resolve (25) for  $R_P$ . This is

$$R_P(f_{RES}) = \frac{2\pi f_{CAR} L_A}{\sqrt{\left(\frac{2\pi f_{CAR} \mu_0 N A H_{MIN}}{U_{CHIP}}\right)^2 - \left[1 - \left(\frac{f_{CAR}}{f_{RES}}\right)^2\right]^2}} \quad (27)$$

and for the chip internal DC current

$$I_{DC} = \frac{U_{CHIP} - U_{DROP}}{R_T} \quad (28)$$

This consideration can also be used, to calculate current available from different antenna sizes mentioned in [13]. For the chip manufacturer or the system integrator this allows to estimate the available current for chip internal operation, e.g. cryptography, if also the voltage drop on the integrated rectifier and other losses are taken into account (so the available DC current for the digital part is less than the AC current at the antenna connection). Interestingly, and different to the opinion of some publications, the antenna quality factor is not very relevant in this context and can even be quite low, e.g. close to 25 (depending on the chip  $R_P$ ). It is the relation of inductance and capacitance, which matters. In fact, less inductance (and more capacitance to result at equal resonance frequencies) allows to achieve higher chip currents, of course on the expense of increased loading and de-tuning of the reader.

### B. Loading Effect

Load modulation is depending on the quasi-static loading effect, as this loading is changed dynamically with the subcarrier frequency between two states. To represent this loading effect in a general way is difficult since accurate estimations of the exact geometries for a specific reader and transponder antenna have to be taken into account. Consequently the best way to model the transponder loading without geometry is to use the magnetic momentum  $M_D$ .

$$M_D = N \cdot A \cdot I \quad (29)$$

where  $A$  is the average antenna area,  $N$  is the number of turns and  $I$  is the current in one turn. If we use again the simplified equivalent circuit of fig. 5, the current in the inductor is given by

$$I = \frac{U}{Z} \rightarrow I_L = \frac{U_C - U_i}{j\omega L_A}. \quad (30)$$

Using our expression for the induced voltage (15), expressed in a different way

$$U_i = -j\omega \mu_0 A N H, \quad (31)$$

this current can be re-written as

$$I_L = \frac{U_i}{j\omega_{CAR} L_A} \cdot \left[ \frac{-jQ_T \frac{\omega_{RES}}{\omega_{CAR}}}{1 + jQ_T \left( \frac{\omega_{CAR}}{\omega_{RES}} - \frac{\omega_{RES}}{\omega_{CAR}} \right)} - 1 \right]. \quad (32)$$

Finally we find the current in the inductor as

$$I_L = \frac{\mu_0 ANH}{L_A} \cdot \frac{1 + jQ_T \frac{\omega_{CAR}}{\omega_{RES}}}{1 + jQ_T \left( \frac{\omega_{CAR}}{\omega_{RES}} - \frac{\omega_{RES}}{\omega_{CAR}} \right)}. \quad (33)$$

Using this current, the magnetic momentum of the transponder is given by

$$M_T = NI_L A. \quad (34)$$

#### IV. OPTIMIZING DESIGN FOR SMALLER ANTENNAS

To optimize the analogue performance of transponders with smaller antennas, we have to focus on energy and load modulation taking into account the previous considerations.

For the energy aspect, we can start with a simple consideration: If the available loop area is reduced by half, this could be compensated with an increase in the number of turns by 2 to achieve the same induced voltage, as  $U_i \sim N$  according eq. (16). But we are working with a resonant system, so if the capacitance of the chip has a fixed value, then the inductance needs to have an equal value to achieve the same resonance frequency for a smaller antenna. However, from  $L \sim N^2$  according eq. (8), it is obvious that both conditions cannot be met at the same time.

There is a practical solution, if energy is not the most limiting factor. High quality low power chip design allows to use resonance frequencies which are higher than the carrier frequency, a typical recommendation is 16 MHz, for class 1 antennas. Although a higher resonance frequency means an increase in the H-field required for transponder operation, it leaves room for detuning of the resonance caused by close coupling to other cards with similar antennas (which may happen with several contactless cards in one pocket) and so gives the Proximity system robustness. For smaller antennas like class 2 it is then possible to shift the resonance frequency to a lower value closer to the carrier (e.g. 13.9 MHz), as the chance for detuning due to high coupling is less for smaller antennas. This allows a similar energy situation for the chip.

However, more important than energy is the load modulation aspect. As the area and the coupling to larger reader antennas decreases, the transponder antenna current must be increased. In this context,  $Q_T$  is most important to consider. Keeping the loss power constant, the energy must be increased. There are two options:

- increasing the current by an increase of  $C_T$ , or
- increasing the voltage of the resonant circuit.

To increase the antenna voltage, the regulated transponder DC voltage could be increased. However, as the memory size requires a majority of the silicon area for these

chips, there is a trend towards smaller structure scales in integration to allow a small die area with huge memory volume to be competitive in price on the market. Smaller scales also mean less operating voltage and in addition, the loss power increases with voltage and may cause a thermal problem for operation at high H-field strengths, so this may not be a future-proof approach.

TABLE III. SYSTEM PARAMETERS OF ISO/IEC14443 CHIPS

Parameter	Chip 1	Chip 2
Capacitance in pF	17	76
min. voltage in V (rms)	2.5	2.5
Shunt resistance in $\Omega$	1000	1000

For objects like watches, a network of external components can be a good option. A capacitor in series between chip and antenna can transform a higher impedance antenna to a lower impedance chip [15]. Unfortunately such a solution cannot be integrated with standard processes, as the contact pad can get a negative voltage to chip ground in operation, which would activate parasitic transistors.

So it remains an option to increase the capacitance and to decrease the number of antenna turns and coil inductance, to achieve higher loading at equal resonance frequency. To show the effect, we can use the two antenna designs of fig. 3 and 4 and combine them with a typical ISO/IEC14443 chip. System parameters for such chips are given in tab. 3.

Using (25), figure 6 shows the energy situation depending on resonance frequency. The class 1 antenna inner area is  $0.00236 \text{ m}^2$ , and for class 2 it is  $0.00145 \text{ m}^2$ . As can be seen, the energy situation for the two different SmartCard antennas are similar, but the more sharp resonance condition for the class 2 antenna requires a smaller tolerance window.

Measurement proofs, the minimum operating H-field for chip 1 and the full-size antenna at 15.9 MHz resonance frequency is  $0.806 \text{ A/m}$ , while for chip 2 and the half-size antenna at 13.9 MHz it is  $0.815 \text{ A/m}$ . If we use (24), the transponder system Q-factor at minimum H-field for the full-size antenna is about 2.1, while for the half-size antenna it is about 7.

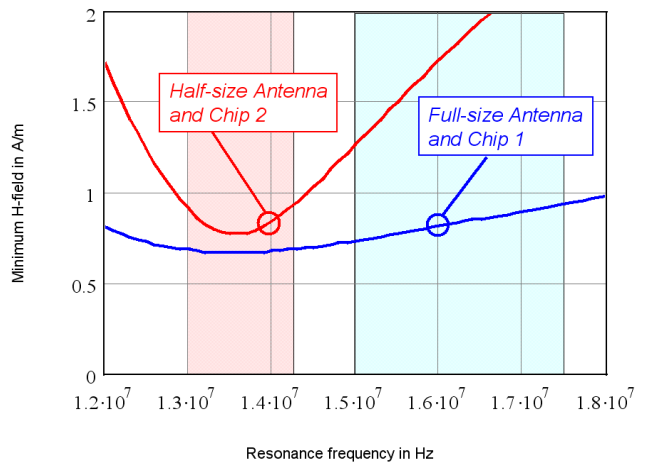


Figure 6. Minimum H-field required for operation.

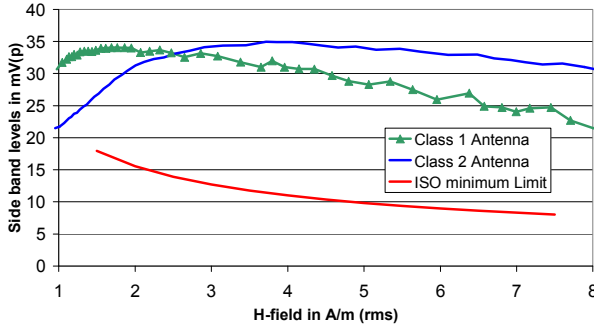


Figure 7. Load modulation measured for SmartCards with full size (class 1) and half-size (class 2) antenna and chips with described properties.

Using (33) we can also compare the current in one antenna turn, which is for the full-size antenna about 5.1 mA, while for the half-size antenna it is about 17.1 mA. And finally, the magnetic momentum for the full-size antenna is equal to the momentum of the half-size antenna, about 72  $\mu\text{Am}^2$  in both cases.

The magnetic momentum is related to the card loading to the reader, which also depends on reader antenna Q-factor and coupling between the antennas. For load modulation, the system Q-factor is modulated on the transponder side (by means of  $R_T$ ), between the highest value, which we have calculated and which also results in highest loading, and a lower value. Load modulation for the two examples as measured in frequency domain with an ISO/IEC10373-6 test bench [14] is shown in fig. 7.

## V. DISCUSSION AND CONCLUSION

Transponder properties at the air interface (as specified in the Proximity base Standard ISO/IEC14443) can be adjusted by proper antenna design on the expense of the tolerance window width. In fact it is possible to achieve equal conditions for a SmartCard chip for energy and load modulation with small antennas than with full-size antennas. Obviously this cannot be achieved by keeping the total area constant (by an increase in the number of turns around a smaller area) on the expense of a lower resonance frequency, it also can not be achieved by an increase of turns compensated by a decrease in capacitance to keep the resonance frequency constant (as it is the opinion in some publications), but it can be achieved by a change in the relation between inductance and capacitance in favor of the capacitance. This means a reduced number of turns of the loop antenna, compensated by increased capacitance, for the practical frame condition of voltage limited transponders. This additional capacitance can be integrated in some antenna technologies (like etched, galvano or printed antennas), e.g. in the conductor-crossing or for a double-sided design. Or it can be integrated in the chip, which allows also to use embedded wire antennas. So for smaller antennas, the main challenge is to increase the system Q-factor (not to confuse with the antenna Q-factor, determined by losses for a given inductance). As the typical reader antenna will be larger than the transponder antenna, the

reduced coupling between reader and transponder, resulting in reduced load modulation can also be compensated by an increased loading due to the more sharp resonance in the transponder system. A drawback is of course, less parameter tolerances can be accepted and more accurate models are required for small antenna design. The equations provided in this document, derived from well-known fundamental equations allow to adjust the SmartCard transponder to this field of requirements.

## REFERENCES

- [1] J. Clerk Maxwell, *A Treatise on Electricity and Magnetism*, 3rd ed., vol. 2. Oxford: Clarendon, 1892.
- [2] Y. Lee, "Antenna Circuit Design for RFID Applications", AN710, Microchip, 2003.
- [3] H. Witschnig, E. Sonnleitner, J. Bruckbauer, E. Merlin, "Eigenvalue Analysis of Close Coupled 13.56 MHz RFID Labels", IEEE MTT-S, International Microwave Symposium, ISBN: 0-7803-9542-5, 2006.
- [4] C. Reinhold, P. Scholtz, W. John, U. Hilleringmann, "Efficient Antenna Design of Inductive Coupled RFID Systems with High Power Demand", Journal of Communications, Vol. 2, No 6, Nov. 2007.
- [5] H. Witschnig, E. Merlin, "Modeling of Multilabel Scenarios of 13.56 MHz RFID Systems", ISBN 978-87487-006-4, EuMC 2008.
- [6] K. S. Leong, M. L. Ng, P. H. Cole, "Investigation on the Deployment of HF and UHF RFID Tag in Livestock Identification", Proc. of 2007 IEEE Antennas & Propagation Society International Symposium.
- [7] ——, "Antenna design of HF-RFID tags with high power requirement," in Proceedings of the 19th International Conference on Herzian Optic and Dielectrics (OHD), pp. 93–98, September 2007.
- [8] K. Fotopoulou, B. W. Flynn, "Optimum Antenna Coil Structure for Inductive Powering of Passive RFID Tags", 2007 IEEE International Conference on RFID.
- [9] S. Cichos, "Verfahren zur Modellierung von planaren Spulen für den Entwurf und die Optimierung von Antennenplatten induktiv gekoppelter RFID-Transponder", Dissertation, TU Berlin, 2006.
- [10] K. O. Soffke, "Modellierung, Simulation und Entwurf induktiv gekoppelter Transpondersysteme", Dissertation, TU Darmstadt, 2007.
- [11] R. Szoncsó "RFID Antenna Sizes", diploma thesis at TU Graz, 2007.
- [12] H. Zangl, T. Bretterklaiber, "Limitations of Range of Operation and Data Rate for 13,56 MHz Load Modulation Systems", Proc. Eurasip 2007.
- [13] M. Gebhart, W. Eber, W. Winkler, D. Kovac, H. Krepelka: "From Power to Performance in 13.56 MHz Contactless Credit Card Technology", IEEE DOI 10.1109/ CSNDSP.2008.4610746, pp. 301-305, 2008.
- [14] M. Gebhart, S. Birnstingl, J. Bruckbauer, E. Merlin: "Properties of a test bench to verify Standard Compliance of Proximity Transponders", IEEE DOI 10.1109/ CSNDSP.2008.4610794, pp. 306-310, 2008.
- [15] M. Gebhart, R. Szoncsó, M. Muenzer, "Improving contactless technology by increase of transponder load modulation with serial capacitor", MELECON 2010.
- [16] X. Qing, Z. N. Chen, "Characteristics of a metal backed Loop Antenna and its application to a High Frequency RFID Smart Shelf", Antennas & Propagation Magazine, Vol. 51, Issue 2, pp. 26 – 38, 2009.
- [17] T. W. H. Fockens, "System model for Inductive ID systems", Nedap, 2000.
- [18] K. Finkenzeller, *RFID-Handbuch*, 3. Auflage, ISBN 3-446-22071-2, Hanser, 2002.